Available online at www.sciencedirect.com
SCIENCE DIRECT®

ELSEVIER

Polymer 44 (2003) 7545–7556

polymer

www.elsevier.com/locate/polymer

Polymer matrix degradation and color formation in melt processed nylon 6/clay nanocomposites

T.D. Fornes, P.J. Yoon, D.R. Paul*

Department of Chemical Engineering and Texas Materials Institute, The University of Texas at Austin, Austin, TX 78712, USA

Received 19 June 2003; accepted 10 September 2003

Abstract

Nylon 6 nanocomposites based on various quaternary alkyl ammonium organoclays were prepared by melt processing using a twin screw extruder. Dilute solution viscosity techniques were used to evaluate the level of polymer molecular weight degradation experienced during nanocomposite compounding; whereas colorimeter techniques were used to document color formation. In general, a significant reduction in nylon 6 matrix molecular weight was observed, which is believed to stem, in part, from reaction(s) between the surfactant of the organoclay and the polyamide chains. The level of degradation depends on both the type of nylon 6 material used and the surfactant chemistry in the organoclay. For a given organoclay, nanocomposites based on high molecular weight nylon 6 materials experience more matrix degradation, as well as color formation, than those based on low molecular weight materials; this is believed to arise from increased exposure of the organoclay surface to the nylon 6 owing to increased platelet exfoliation. Different organoclays lead to different levels of polymer degradation and color formation, depending upon the level of unsaturation present in the organic surfactant; the higher the number of double bonds the greater the degradation and the deeper the color formation. The primary mechanism of degradation is believed to be thermo-oxidative. Melt mixing of nylon 6 with model compounds, long-chain alkenes, shows that the same mode of degradation i.e. via double bonds can be replicated. In addition to unsaturation effects, the presence of hydroxyl–ethyl groups, opposed to methyl groups, in the organoclay surfactant, results in more color. Isothermal thermogravimetric analysis (TGA) was conducted on the organoclays to determine if thermal stability was a cause of molecular weight degradation; although, this relationship does not seem to exist, a direction correlation is observed between the organoclay degradation and nanocomposite modulus, or indirectly level of exfoliation. Use of antioxidant was found to reduce the amount of molecular weight loss. All evidence suggests that morphology and physical properties of nanocomposites formed from nylon 6 are not measurably affected by the reactions that lead to molecular weight degradation or color formation.

Keywords: Nylon 6; Nanocomposites; Degradation

1. Introduction

An attractive approach for forming nanocomposites is by melt mixing the polymer of interest with an organically modified clay. Nanocomposites based on thermoplastics synthesized by other approaches, e.g. in situ polymerization, are generally fabricated into useful shapes by some melt processing technique. Thus, for polymers that require high melt processing temperatures, the thermal stability of the organic component of the modified clay, often alkyl ammonium compounds, becomes a significant issue for a variety of reasons.

Thermogravimetric analysis (TGA) shows that the organic component of organoclays begins to breakdown at temperatures as low as 180 °C under non-oxidative environments and significant degradation occurs just above this temperature. An extensive overview of the degradation of alkyl ammonium montmorillonite organoclays has been given by Xie et al. [1,2]. Unfortunately, these degradation temperatures may be exceeded during the melt processing of many polymers. As noted by Xie et al., such degradation may affect the thermodynamics of polymer melt intercalation, due to chemical changes in surfactant structure, and thus alter the level of platelet exfoliation and interfacial bonding, which influence physical and mechanical properties. In addition, the decomposition of the surfactant may produce unwanted side reactions with the

---

* Corresponding author. Tel.: +1-512-471-5392; fax: +1-512-471-0542.
E-mail address: drp@che.utexas.edu (D.R. Paul).

0032-3861/$ - see front matter © 2003 Elsevier Ltd. All rights reserved.
doi:10.1016/j.polymer.2003.09.034

polymer matrix. Given the above, a better understanding of organic modifier degradation and how it affects nanocomposite formation is needed.

Some recent investigations have addressed the issue of organic modifier stability during melt processing. For example, VanderHart et al. [3,4] estimated from NMR measurements that a considerable portion of the quaternary alkyl ammonium component is depleted during melt processing of nylon 6 nanocomposites. They concluded that the cause of the degradation is a combination of temperature and mechanical shear that is encountered during processing. The instability of the organoclay can also have adverse affects on the polymer itself. Matabayas and Turner [5] found that significant polymer matrix degradation occurs during the extrusion of poly(ethylene terephthalate) (PET)–organoclay mixtures. Yoon et al. [6] observed similar effects when processing polycarbonate–organoclay mixtures. In addition, considerable color was generated in the nanocomposites and was found to be function of clay platelet exfoliation, extruder residence time, and the structure of the organic surfactant used to form the organoclay.

Recent rheological studies on nanocomposites provide implicit evidence for polymer molecular weight degradation. For instance, Fig. 1 shows that the melt viscosity of nylon 6 nanocomposites, as measured by a capillary rheometer [7,8], is lower than that of the pure polyamide itself. Similar results have been reported for nanocomposites based on copolymers of dimethylsiloxane and diphenylsiloxane [9], dimethylsiloxane [9], and polycarbonate [6], in addition to those based on nylon 6 [7,8,10]. Such reductions in viscosity are often attributed to alignment of the clay platelets parallel to the direction of the applied shear [11]; however, the possible contribution of molecular weight degradation cannot be ignored in such observations.

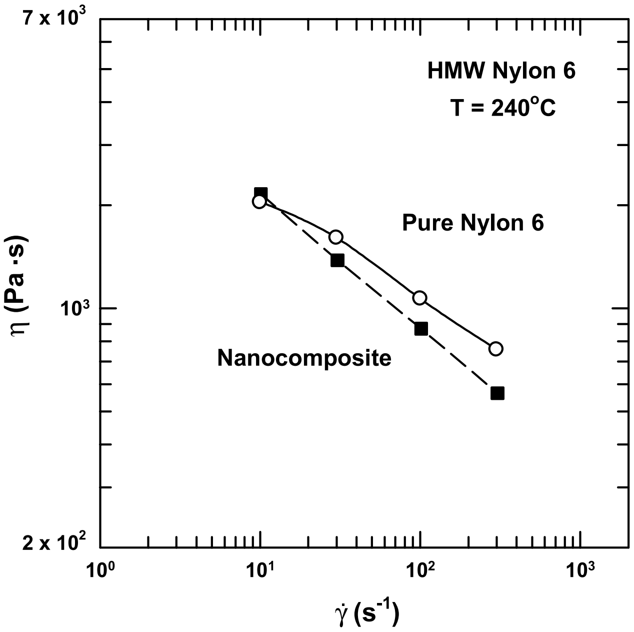

Fig. 1. The influence of shear rate on steady shear viscosity for high molecular weight nylon 6 (HMW) and a nanocomposite containing 3.2 wt% MMT made from organically modified montmorillonite $(HE)_2M_1R_1$ by melt processing. Viscosity measurements were made at 240 °C using a capillary rheometer. Specific details of these materials, experimental procedures, and related results are given elsewhere [7,8].

The objective of this paper is to examine the level of polymer degradation and color formation experienced during the melt processing of nylon 6–organoclay nanocomposites. Specifically, degradation and color development are evaluated for nanocomposites made from different molecular weight grades of nylon 6 and different quaternary alky ammonium organoclays. Attempts to simulate and minimize the degradation process through the use of model compounds and commercial antioxidants, respectively, are discussed. The effect of antioxidant on nanocomposite morphology and mechanical properties is also addressed.

2. Experimental

2.1. Materials

Three commercial nylon 6 materials from Honeywell with low (Capron 8202), medium (Capron B73WP), and high (Capron B135WP) molecular weights were used in this study and will be referred to as LMW, MMW, and HMW, respectively. Organoclays based on montmorillonite (see Table 1) were supplied by Southern Clay Products. Other detailed studies on the processing and performance of the resulting nanocomposites can be found elsewhere [7,8,12,13]. A simple nomenclature system is used to describe the substituents on the nitrogen of the organic modifier in the clay. The symbol M represents methyl, HE represents 2-hydroxy-ethyl, and C^*, T and R represent units derived from the natural products coca, tallow and rapeseed, respectively, each consisting of an average distribution of saturated and unsaturated hydrocarbons, as shown in Table 2. The hydrogenated form of T, designated here as HT, still contains a small amount of unsaturation.

Model compounds, *trans*-7-tetradecene (TTD) and *cis*-9-henieocene (CH), purchased from Sigma-Aldrich, in addition to the alkyl ammonium chloride of $(HE)_2M_1R_1$ obtained from Southern Clay Products, were used to simulate the thermo-oxidative degradation of nylon 6 that occurs during the extrusion of nylon 6–organoclay mixtures. Three types of antioxidant materials, Irganox® 1171, a blend of a phosphite and a sterically hindered phenolic-amide from Ciba Specialty Chemicals, Inc., Irganox® 245, a sterically hindered phenolic-ether also from Ciba, and Wingstay® 29, a derivative of a diphenyl-amine from Goodyear, were chosen for this work. These selections were based on manufacturer recommendations and data available in the literature for their ability to minimize polyamide molecular weight degradation during

Table 1
Organoclays used in this study

Organoclay[a]	SCP designation[b]	Chemical structure	Specifications[c]
$(HE)_2M_1R_1$	Experimental	Bis(2-hydroxy-ethyl)methyl rapeseed ammonium montmorillonite	95 MER Organic content = 34.1 wt% d_{001} spacing = 18.0 Å L^* = 93.3
$(HE)_2M_1C_1^*$	Experimental	Bis(2-hydroxy-ethyl)methyl coco ammonium montmorillonite	95 MER Organic content = 26.4 wt% d_{001} spacing = 15.2 Å L^* = 93.9
$(HE)_2M_1T_1$	Cloisite® 30B	Bis(2-hydroxy-ethyl)methyl tallow ammonium montmorillonite	90 MER Organic content = 31.5 wt% d_{001} spacing = 17.9 Å L^* = 93.5
M_3T_1	Experimental	Trimethyl tallow quaternary ammonium montmorillonite	95 MER Organic content = 29.1 wt% d_{001} spacing = 17.8 Å L^* = 94.1
$M_3(HT)_1$	Experimental	Trimethyl hydrogenated-tallow ammonium montmorillonite	95 MER Organic content = 29.6 wt% d_{001} spacing = 18.0 Å L^* = 94.1

[a] The substituents on the quaternary ammonium compounds used to form the above organoclays are identified in the following shorthand notation: C*, coco; R, rapeseed; T, tallow; HT, hydrogenated-tallow; HE, 2-hydroxy-ethyl; M, methyl. Coca, rapeseed and tallow are natural products composed predominantly of unsaturated C_{12} alkyl chains (48%), C_{22} alkyl chains (45%), and C_{18} alkyl chains (65%), respectively.

[b] Commercial designations provided by Southern Clay Products.

[c] The organic loading is a quantity describing the number of milliequivalents of amine salt used per 100 g of clay (MER) during the cationic exchange reaction with sodium montmorillonite. The wt% of organic component on the final organoclay was determined by high temperature residual ash measurements. The basal spacing corresponds to the characteristic Bragg reflection peak (d_{001}) obtained from a powder WAXS scan of the organoclay.

Table 2
Hydrocarbon percent distribution within natural products used to form the organic modifier on the clay

Carbon no.[a]	Coconut C*	Tallow T	Rapeseed R	Hydrogenated tallow HT
6	0.5			
8	7.0			
10	6.0			
12	48.0			
14	19.0	3.5		3.5
14′		1		
15		0.5		0.5
16	9.0	25.3	4	31
16′		4	0.3	
17		2.5		1
18	3.0	19.4	1	61
18′	6.0	40.8	15	3
18″	1.5	2.5	14.1	
18‴			9.1	
20		0.5	1	
20′			10	
22			0.8	
22′			45.1	

Data obtained with permission from Akzo-Nobel.

[a] The prime symbol, ′, represents an unsaturated hydrocarbon, e.g. 18′, corresponds an 18 carbon membered hydrocarbon that contains one double bond, whereas 18″ and 18‴ represent hydrocarbons containing two and three double bonds, respectively.

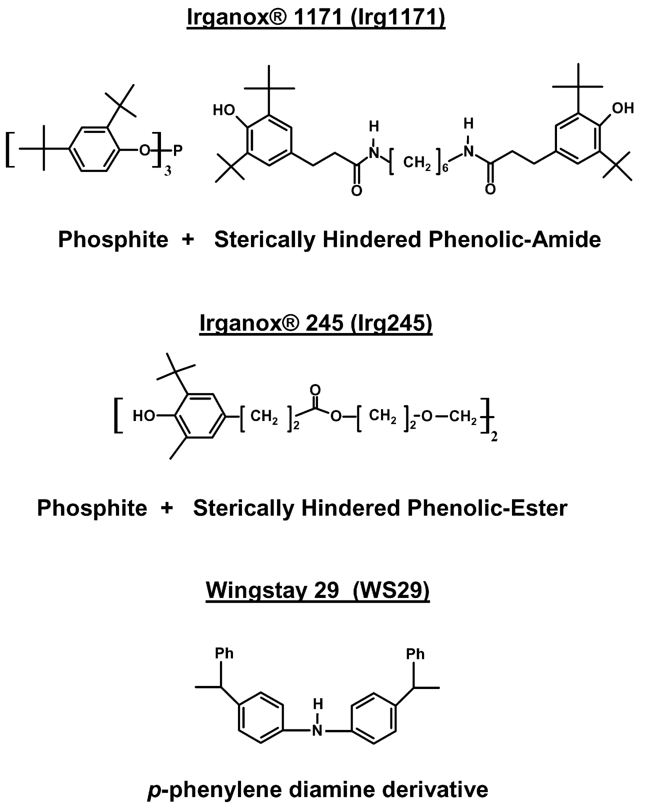

Fig. 2. Chemical structures of commercial antioxidants used in this study.

melt processing [14]. The structures of each antioxidant and the designations used here are shown in Fig. 2.

2.2. Melt processing

Nanocomposites were formed by extruding mixtures of nylon 6 pellets and organoclay powder at 240 °C using a Haake twin screw extruder (diameter = 30 mm, *L*/*D* = 10), as previously described [7,8,12]. Composites based on the $(HE)_2M_1R_1$ organoclay were independently processed with each of the three nylon 6 materials; whereas, only HMW nylon 6 was used in combination with the other organoclays. Following extrusion, the amount of montmorillonite (MMT) in each nanocomposite was determined by placing pre-dried extruded pellets in a furnace at 900 °C for 45 min and weighing the remaining MMT ash. A correction for loss of structural water was made in the calculation [7,8].

Model compound and antioxidant studies were conducted using the HMW nylon 6 material. In the model compound experiments, nylon 6 pellets were first coated with either TTD (0.86 wt%) or CH (1.29 wt%) and then subsequently extruded under the same conditions as used to make the nanocomposites. Likewise, the alkyl ammonium chloride of $(HE)_2M_1R_1$ (1.56 wt%) was extruded with HMW nylon 6; the quantities of model compound and alkyl ammonium chloride added were based on the molar equivalent of unsaturation (double bonds) present in the $(HE)_2M_1R_1$ derived organoclay used to make a 3.2 wt% MMT nanocomposite. Antioxidant compounds (1 wt%) were independently mixed with HMW nylon 6 pellets and $(HE)_2M_1R_1$ organoclay powder in a 3 L container and subsequently extruded under conditions outlined above.

Nanocomposite pellets obtained from extrusions were injection molded into standard 3.18 mm thick tensile (ASTM D638, Type I) and Izod (ASTM D256) specimens using an Arburg Allrounder 305-210-700 injection molding machine set at a barrel temperature of 260 °C, mold temperature of 80 °C, injection pressure of 70 bar, and a holding pressure of 35 bar. It is important to note that prior to any melt processing step, all polyamide containing materials were dried under vacuum at 80 °C for a minimum of 16 h.

2.3. Characterization

Intrinsic viscosities (IVs) were determined on dried extruded pellets using a size 200 Cannon-Fenske viscometer (ASTM D446) at 24.6 °C using dilute solutions of nylon 6 (0.4 g/dL) in *m*-cresol. The number average molecular weight, $\bar{M}_n$, for each sample was calculated using the correlation developed by Tuzar and Kratchovil [15] with *m*-cresol as the solvent at 25 °C,

$$[\eta] = 5.26 \times 10^{-4}\, \bar{M}_w^{0.745} \tag{1}$$

Assuming that each sample has the most probable distribution of molecular weight, the values of $\bar{M}_n$ were calculated by dividing $\bar{M}_w$ obtained from Eq. (1) by two. The IVs obtained here on the virgin materials agree well with previously reported values from this laboratory [16]. Nanocomposite viscosity measurements were made using unfiltered solutions and calculated on the basis of polymer mass (not including clay). The clay is assumed to have a negligible effect on the nanocomposite viscosity; experiments using very dilute *m*-cresol-organoclay solutions revealed marginal differences in flow times compared to pure *m*-cresol.

Color levels were measured on injection molded specimens in the reflection mode using a colorimeter, MICRO S-5 Brightmeter, equipped with a quartz-tungsten halogen lamp. The chromaticity coordinates, L^*, a^* and b^*, were computed from CIE tristimulus red, green and blue responses using a series of formulae described in ASTM E313; L^*, which represents the darkness of color in the chromaticity coordinates [17], is used to quantify differences in color between the various nanocomposites.

Isothermal TGA was carried out on pure organoclays to determine if organoclay stability correlated with the level of polyamide degradation experienced during extrusion. Isothermal experiments were conducted using a Perkin–Elmer TGA7 at 240 °C in an air atmosphere at a gas flow rate of 50 mL/min according to ASTM E1131. All organoclays were dried overnight under vacuum at 80 °C prior to thermal analysis.

Wide angle X-ray scattering (WAXS) scans were conducted in the reflective mode on selected nanocomposite Izod bars at a scan rate of rate of 1°/min using a Sintag XDS 2000 diffractometer using Ni filtered CuK_α X-ray radiation ($\lambda = 1.54$ Å). The bars were orientated such that the incident beam reflected off the major surface of the bar, as previously described [7,8].

Tensile tests were performed according to ASTM D638 on tensile specimens using an Instron model 1137. Modulus and yield strength were determined using an extensometer at a test rate of 0.51 cm/min; whereas, elongation at break was measured at speeds of 0.51 and 5.1 cm/min from total crosshead travel assuming a gauge length of 9.04 cm. Tensile properties reported here represent an average value of six specimens; relative error was typically 4% for modulus, 1% for yield strength, and 5–25% for elongation at break [7,8].

3. Results and discussion

3.1. Nylon 6–$(\mathrm{HE})_2\mathrm{M}_1\mathrm{R}_1$ nanocomposites

Previous studies conducted in this laboratory demonstrated that the higher molecular weight grades of nylon 6, i.e. MMW and HMW, led to better exfoliation of the organoclay during melt extrusion than those based on the lowest molecular weight material, i.e. LMW [7,8,12]; this was evident in both the morphology, as determined by WAXS and transmission electron microscopy (TEM), and mechanical properties. Composites formed from HMW and MMW nylon 6 were well-exfoliated, consisting largely of individually dispersed platelets; whereas, those based on the LMW matrix revealed a mixed morphology, containing both agglomerates of multi-layered stacks and individually dispersed platelets. The superior morphology of the MMW- and HMW-based nanocomposites translated into better reinforcement, as evident from significantly higher composite moduli and yield strengths.

During processing, several noteworthy rheological effects were observed. For example, the energy required to extrude the nanocomposites containing ~3 wt% MMT or less was markedly less than the energy for the respective virgin nylon 6 materials alone. Also, nanocomposites based on the higher molecular weight polyamides, in general, exhibited more pronounced rheological changes. Furthermore, the cycle time needed to injection mold tensile and Izod specimens were often less than the time needed for the pure polyamide materials. As mentioned above, degradation of the polymer matrix during extrusion may be part of the reason for these effects; this is a point that demands further attention. Thus, intrinsic viscosity measurements were conducted on these nanocomposite materials.

Table 3 lists the nylon 6 molecular weights obtained from IV measurements for nylon 6 materials and their nanocomposites based on $(\mathrm{HE})_2\mathrm{M}_1\mathrm{R}_1$ organoclay. Regardless of the type of nylon 6, the nanocomposites exhibit significantly lower molecular weights than the respective virgin polymer. Extrusion of pure nylon 6 accounts for some of this reduction (see Table 3); however, the amount of reduction is far less than that is experienced by the nanocomposites. Moreover, the level of polymer matrix degradation for the HMW nylon 6 case is nearly five times that seen for the corresponding LMW nanocomposite. It should be pointed out that the present extruder, due to its small size, is not vented; therefore, nylon 6–organoclay nanocomposites processed on other systems with vacuum venting may not experience the level of polymer degradation reported here. Ultimately, the degradation is believed to stem from chemical reaction(s) between the organoclay surface and the polyamide. In the case of the higher molecular weight nanocomposite materials, a larger amount of organoclay surface is exposed to the nylon 6 due to increased levels of clay platelet exfoliation. Similar trends have been reported by Matabayas and Turner [5] for melt processed PET–organoclay nanocomposites; increasing the molecular weight of PET lead to more severe degradation than for a lower molecular grade. In addition, the level of PET degradation increased with increasing clay concentration, regardless of the original PET molecular weight used. More recently, Yoon et al. [6] found that greater dispersion of the organoclay within polycarbonate also leads to higher matrix molecular weight reduction. These results, as well as those presented here, provide a plausible explanation for the unexpectedly low viscosities encountered at high shear rates, as mentioned earlier.

The extent of color formation is also documented for $(\mathrm{HE})_2\mathrm{M}_1\mathrm{R}_1$ nanocomposites based on nylon 6, as shown in

Table 3
Molecular weight results for extruded nanocomposites based on $(\mathrm{HE})_2\mathrm{M}_1\mathrm{R}_1$ organoclay and nylon 6 materials

Material	$\bar{M}_n$[a] (kg/mol)	$\bar{M}_n$ reduction[b] (%)
Matrix: LMW nylon 6		
Virgin LMW	16.8	–
Extruded LMW	16.6	1.2
LMW-$(\mathrm{HE})_2\mathrm{M}_1\mathrm{R}_1$ nanocomposite[c]	15.9	5.4
Matrix: MMW nylon 6		
Virgin MMW	22.5	–
Extruded MMW	21.3	5.2
MMW-$(\mathrm{HE})_2\mathrm{M}_1\mathrm{R}_1$ nanocomposite[c]	17.1	24.0
Matrix: HMW nylon 6		
Virgin HMW	30.1	–
Extruded HMW	28.2	6.3
HMW-$(\mathrm{HE})_2\mathrm{M}_1\mathrm{R}_1$ nanocomposite[c]	22.5	25.2

[a] Molecular weights were determined via intrinsic viscosity measurements.

[b] The percent reduction is relative to the virgin polyamide molecular weight.

[c] Nanocomposites contain ~3.2 wt% MMT.

Fig. 3. The color index value (L^*) listed in this figure gives a more quantitative description of the depth of nanocomposite color. Fig. 4 shows the effect of MMT content and matrix molecular weight on the level of color generated in $(HE)_2M_1R_1$ nanocomposites; since the color is different for each of the pure extruded polyamides, the nanocomposite color index, L^*_{Nano}, is normalized to its respective extruded matrix color index, L^*_{Ext}. As expected, the level of color intensifies with increasing clay content, evident by lower relative L^* values. Furthermore, the depth of color for the nanocomposites tends to be more pronounced for the higher molecular matrices implying that exposing more organoclay surface to the nylon 6 by exfoliation promotes deeper color formation. To explore this relationship, the modulus of these materials, which is a strong indicator of extent of clay platelet exfoliation, is plotted against relative darkness, as seen in Fig. 5; note this plot includes data having different levels of MMT. Regardless of the nylon 6 material, the data fall on a universal curve, further indicating that, for a given organoclay, a strong correlation between color index and extent of organoclay exfoliation exists.

3.2. Organoclay structure effects

The effect of the structure of the quaternary alkyl ammonium modifier on the matrix molecular weight degradation for extruded nanocomposites is listed in Table 4. These results show that the level of degradation is clearly dependent upon the surfactant with at least two distinct structural effects in evidence. First, HE groups on the surfactant nitrogen result in slightly less polyamide degradation than methyl substituents, as seen by comparing $(HE)_2M_1T_1$ and M_3T_1. Interestingly, this is opposite of the observation for polycarbonate based nanocomposites [6]. Second, hydrogenation of the tallow, i.e. HT, leads to less degradation than the unsaturated tallow form, T; this is

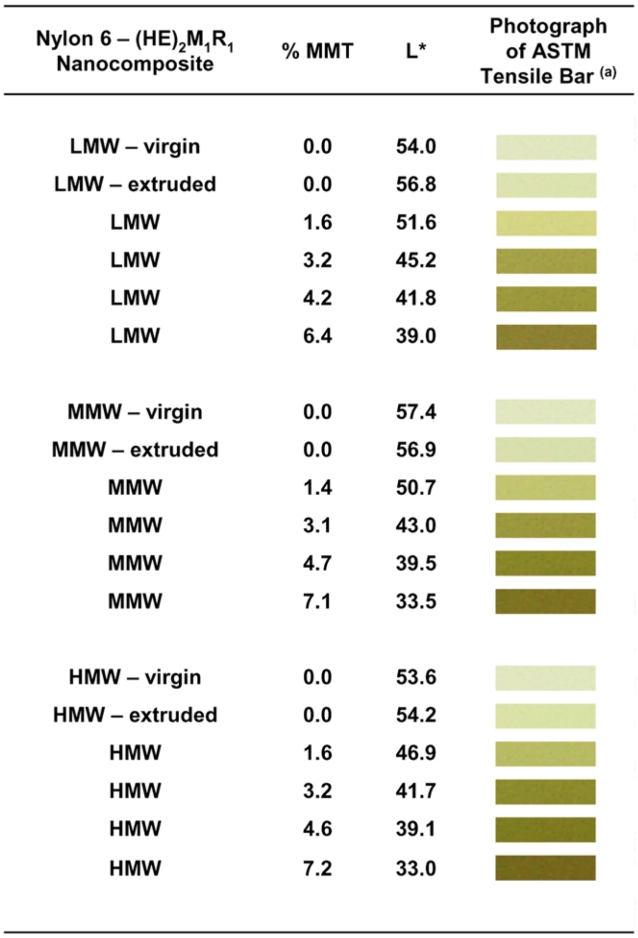

Nylon 6 – $(HE)_2M_1R_1$ Nanocomposite	% MMT	L*	Photograph of ASTM Tensile Bar [(a)]
LMW – virgin	0.0	54.0	▨
LMW – extruded	0.0	56.8	▨
LMW	1.6	51.6	▨
LMW	3.2	45.2	▨
LMW	4.2	41.8	▨
LMW	6.4	39.0	▨
MMW – virgin	0.0	57.4	▨
MMW – extruded	0.0	56.9	▨
MMW	1.4	50.7	▨
MMW	3.1	43.0	▨
MMW	4.7	39.5	▨
MMW	7.1	33.5	▨
HMW – virgin	0.0	53.6	▨
HMW – extruded	0.0	54.2	▨
HMW	1.6	46.9	▨
HMW	3.2	41.7	▨
HMW	4.6	39.1	▨
HMW	7.2	33.0	▨

(a) Photographs were taken on 3.18 mm thick specimens.

Fig. 3. Color formation in various nylon 6 nanocomposites based on $(HE)_2M_1R_1$ organoclay.

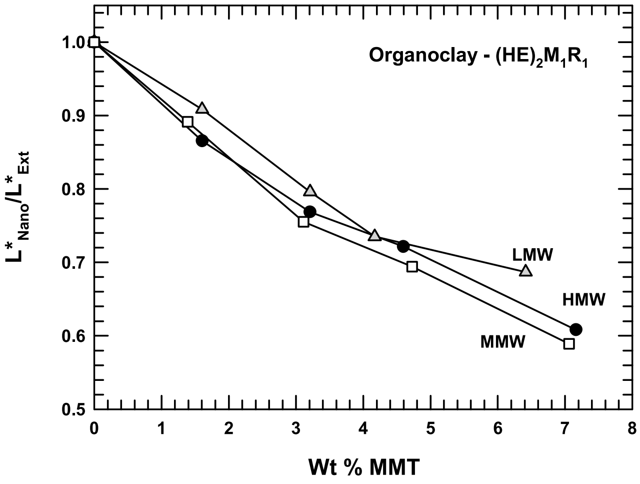

Fig. 4. The effect of MMT content on nanocomposite color index, L^*_{Nano}, normalized by the value extruded nylon 6, L^*_{Ext}. Nanocomposites are based on the $(HE)_2M_1R_1$ organoclay.

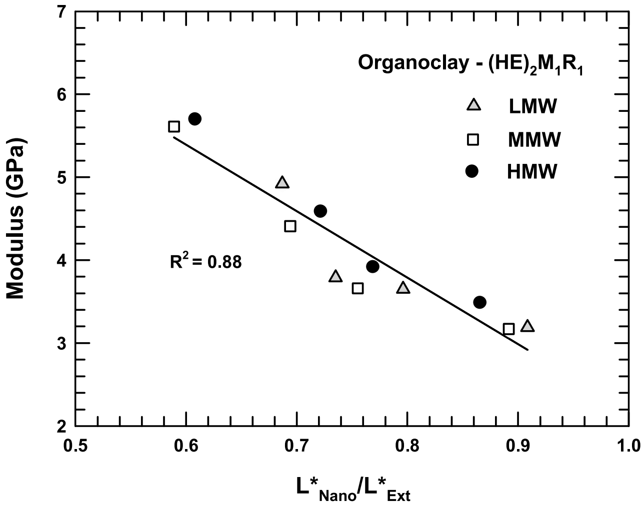

Fig. 5. Relationship between nanocomposite modulus and relative nanocomposite color index for $(HE)_2M_1R_1$ nanocomposites based on LMW, MMW and HMW nylon 6.

Table 4
Effect of organoclay type on nylon 6 matrix molecular weight of extruded nanocomposites based on HMW nylon 6

HMW-organoclay nanocomposite	MMT level (wt%)	$\bar{M}_n$[a] (kg/mol)	$\bar{M}_n$ reduction[b] (%)
Virgin HMW	0.0	30.1	–
Extruded HMW	0.0	28.2	6.3
$(HE)_2M_1R_1$	3.2	22.5	25.2
$(HE)_2M_1C_1^*$	2.9	26.1	13.3
$(HE)_2M_1T_1$	2.8	25.1	16.6
M_3T_1	2.8	24.5	18.6
$M_3(HT)_1$	2.9	26.3	12.6

[a] Molecular weights were determined via intrinsic viscosity measurements.

[b] The percent reduction is relative to virgin HMW.

evident by comparing $M_3(HT)_1$ and M_3T_1. It is known that materials containing double bonds are susceptible to free radical formation under thermo-oxidative conditions [18–21]. In turn, these free radicals can attack the polymer which may result in chain scission, hence a reduction in polymer molecular weight, and, in some cases, affect physical and mechanical properties [19–23]. Thus, the amount of unsaturation should affect the extent of degradation by this mechanism. Using the hydrocarbon distribution information for the natural products used in the synthesis of the organoclay modifiers (see Table 2), the quantity of double bonds present prior to extruding the nanocomposite can be calculated. Fig. 6 shows a direct relationship between the initial level of unsaturation in each nanocomposite and the amount of molecular weight reduction experienced by the nylon 6 matrix. Extrapolation of this plot gives a molecular weight reduction of 12.9% when there are no double bonds present; this is approximately two-fold the level experienced by extruding HMW nylon 6 without any clay. This suggests there are other degradation pathways caused by the organoclay.

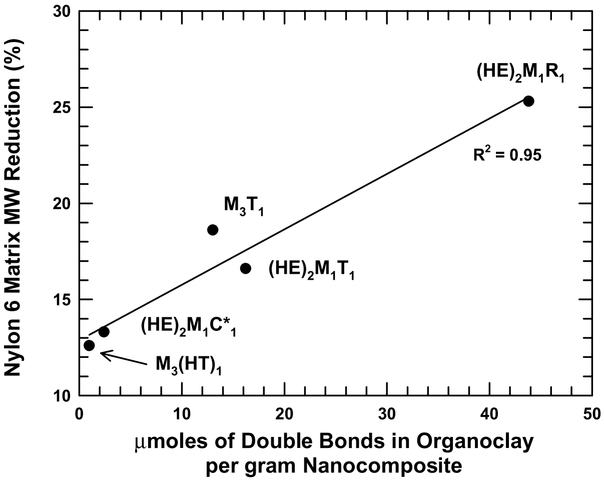

Fig. 6. Influence of unsaturation of the organoclay on the level of nylon 6 matrix molecular weight reduction experienced during melt extrusion of nanocomposites. Nanocomposites were formed from HMW nylon 6 and organoclays listed in Table 1. Unsaturation levels of the natural products used in the formation of the organoclay surfactant are listed in Table 2.

Xie et al. [1] showed that alkyl ammonium organoclays decompose between 200 and 300 °C to produce α-olefins and amines, among other organic species, which is suggestive of the Hofmann elimination mechanism [24]; this mechanism generally occurs when a quaternary ammonium hydroxide or chloride, under high temperatures, is converted into an alkene and an amine, as depicted in Fig. 7(a). However, in the case of organoclays, elimination of the ammonium modifier may result in a substitution of the ammonium linkage on the clay with a hydrogen proton on the β-carbon (see Fig. 7(b)); possible evidence of protons bound to clay surface has been reported by Davis et al. [25]. Ultimately, the α-olefins, by-products, or intermediates produced in this reaction could attack the polymer.

Furthermore, it is well known that the organoclays contain a small fraction of absorbed water, which at high temperatures when processed can cause hydrolysis of the polyamide. Davis et al. [25] reported a significant level of nylon 6 degradation during high temperature melt processing, i.e. at 300 °C, of in situ formed nylon 6 nanocomposites. They proposed that the degradation was largely due to hydrolysis by water from the clay, either bound or from dehydroxylation of the MMT itself. These authors also suggest other mechanisms, such as catalytic degradation caused by unexchanged sodium cations on the surface of the clay.

Thermogravimetric studies with the present organoclays were conducted to determine if the nylon 6 degradation during nanocomposite processing can be related to the measure of surfactant degradation. Isothermal TGA experiments were performed in air at 240 °C in an effort to simulate extruder processing conditions. Fig. 8 shows organoclay surfactant weight loss as a function of time; superimposed on this graph is the extruder residence time distribution (RTD) for HMW nylon 6 [7,8]. The amount of surfactant decomposition observed by TGA is considerable and depends upon surfactant structure; note that the TGA experiment does not include shear effects, which have been claimed to contribute to surfactant instability [3,4]. It is interesting to compare the amount of surfactant degradation to the level nylon 6 molecular weight reduction experienced during nanocomposite extrusion. Specific comparisons of surfactant chemistry show that the organoclay based on $M_3(HT)_1$ appears to be slightly more stable than its unsaturated version, M_3T_1, which parallels the polymer matrix degradation trend seen in the respective nanocomposites (see Table 4) Likewise, replacing methyl groups with HE groups on the nitrogen, i.e. M_3T_1 vs. $(HE)_2M_1T_1$, leads to a more stable organoclay and slightly less polyamide degradation during extrusion. A more quantitative comparison can be made by plotting the level of nylon 6 degradation against surfactant weight at time = 3.4 min (see Fig. 9). This time corresponds to the mean residence time of the extruder; however, it is important to mention that

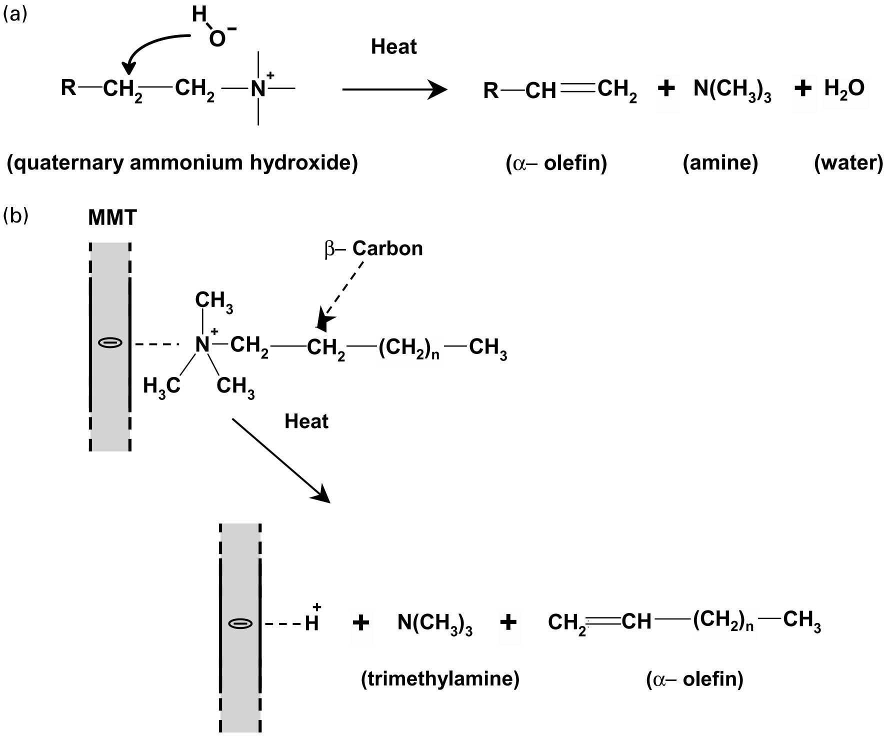

Fig. 7. The Hofmann elimination reaction for quaternary ammonium compounds: (a) general reaction scheme and (b) a proposed scheme for organically modified MMT.

a portion of this time in the extruder is spent heating and melting prior to mixing the organoclay with the polymer, so the organoclay is not at 240 °C for all of this time. In general, Fig. 9 shows no clear relationship between the thermal stability of the organoclay and the final nylon 6 molecular weight measured for the nanocomposites.

Interestingly, a distinct correlation does exist between the nanocomposite modulus and the amount of surfactant remaining in the organoclay at time = 3.4 min, as shown in Fig. 10. Higher levels of surfactant degradation seem to translate into higher nanocomposite moduli; this implies that degradation does not impede the exfoliation process. Moreover, it may aid exfoliation, to a certain degree, by making the clay surface less hydrophobic and, thereby, increasing the affinity between the polyamide chains and the clay; recent investigations conducted on these and similar nylon 6–organoclay nanocomposites concluded that organic modifiers that cover less of the pristine surface of the MMT decreases the number of polyamide–surfactant interactions and increase the number of favorable polyamide-silicate interactions which results in better platelet exfoliation [12]. This conclusion is supported by experimental trends seen in nanocomposite morphology and mechanical properties, and is predicted by thermodynamic

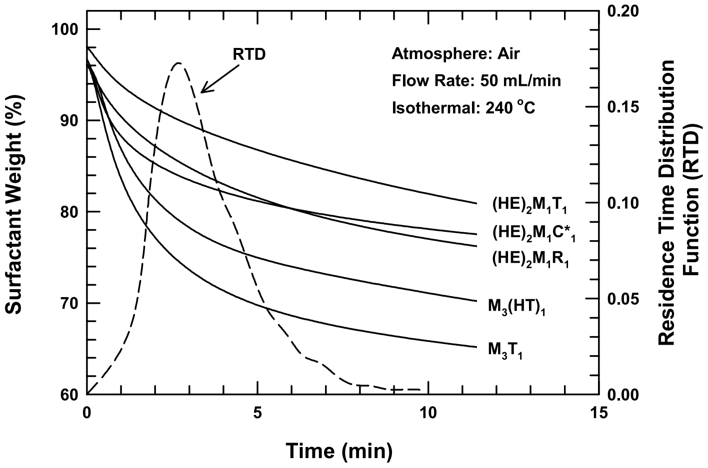

Fig. 8. Isothermal TGA results of pre-dried organoclays obtained in air at 240 °C. Superposed on this graph is a plot the extruder residence time distribution function (dashed line) previously obtained for HMW nylon 6 [7,8].

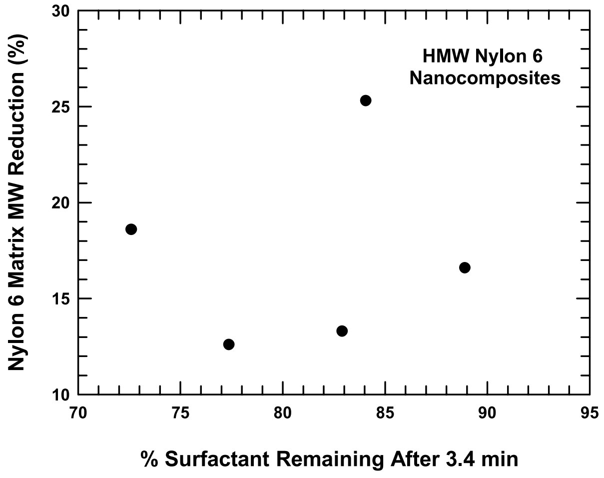

Fig. 9. Plot of nylon 6 molecular weight reduction experienced during the melt extrusion of nanocomposites vs. organoclay surfactant stability. The surfactant stability is represented here by the percent surfactant remaining after 3.4 min (mean residence time of HMW nylon 6 spent in the extruder) as measured by isothermal TGA (see Fig. 8).

models [26–29]. VanderHart et al. [3] determined by solid state NMR that melt processed nylon 6–organoclay nanocomposites with the highest level of platelet dispersion experienced also had the largest amount of surfactant degradation. It was suggested that both a greater exposure of the polymer to surfactant via exfoliation and changes in extrusion conditions, such as increasing the residence time or the level of applied shear, may give more opportunity for degradation. The evidence shown here and elsewhere suggest that degradation does not seem to hinder clay platelet exfoliation in nylon 6; this of course may not be the case in other polymers.

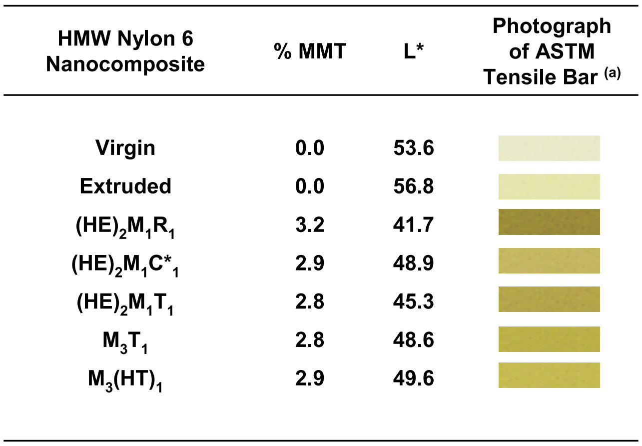

HMW Nylon 6 Nanocomposite	% MMT	L*	Photograph of ASTM Tensile Bar [(a)]
Virgin	0.0	53.6	▨
Extruded	0.0	56.8	▨
$(HE)_2M_1R_1$	3.2	41.7	▨
$(HE)_2M_1C^*_1$	2.9	48.9	▨
$(HE)_2M_1T_1$	2.8	45.3	▨
M_3T_1	2.8	48.6	▨
$M_3(HT)_1$	2.9	49.6	▨

(a) Photographs were taken on 3.18 mm thick specimens.

Fig. 11. The effect of organoclay structure on color formation in HMW nylon 6 nanocomposites.

Organoclay structure also has a noticeable effect on nanocomposite color. Fig. 11 shows color photographs of various nanocomposites. In general, the color developed during melt processing is a function of the color of the pure organoclay, as indicated in Fig. 12. Even though the difference between the color indices of the organoclays is small, a significant difference in nanocomposite color is obtained. Some interesting color effects may be seen in Fig. 11: (1) increasing the length of the alkyl tail from 12 to 18 to 22 carbons, i.e. $(HE)_2M_1C_1^*$ vs. $(HE)_2M_1T_1$ vs. $(HE)_2M_1R_1$, respectively, results in deeper nanocomposite color, (2) the presence of HE groups on the surfactant nitrogen as compared to methyl groups, i.e. $(HE)_2M_1T_1$ vs. M_3T_1, leads to more nanocomposite color, and (3) hydrogenation of the tallow results in less color formation, evident in the comparison of $M_3(HT)_1$ vs. M_3T_1. The latter trend may be a consequence of nylon 6 degradation, given the trend seen in Fig. 6. Several studies [30–32] have shown that the thermo-oxidation of nylon 6, which is proposed here, leads to significant discoloration, e.g. yellowing. The correlation of nanocomposite color index with extent of nylon 6 matrix degradation seen in Fig. 13 provides plausible evidence of this. Polymer degradation may also explain the trend

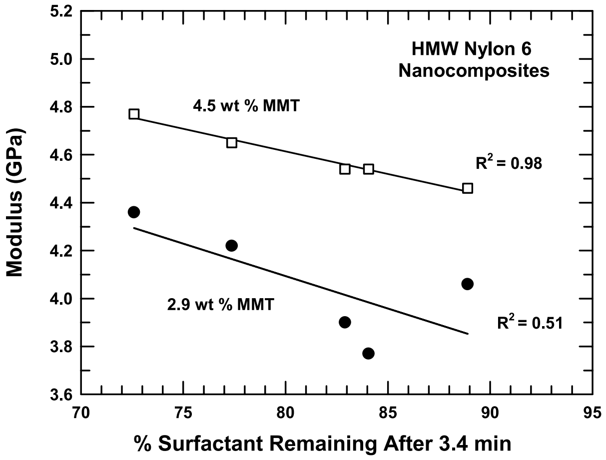

Fig. 10. The influence of organoclay surfactant stability on nanocomposite modulus. The surfactant stability is represented here by percent surfactant remaining after 3.4 min as measured by isothermal TGA (see Fig. 8). The time of 3.4 min is the mean residence time of HMW nylon 6 spent in the extruder.

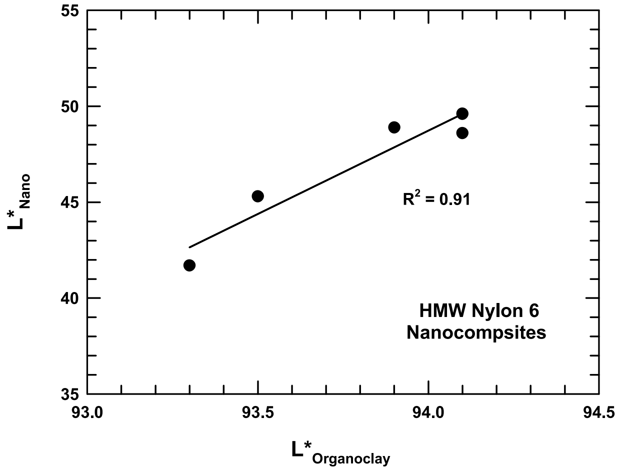

Fig. 12. Relationship between nanocomposite color index, L^*_{Nano}, and organoclay color index, $L^*_{\text{Organoclay}}$.

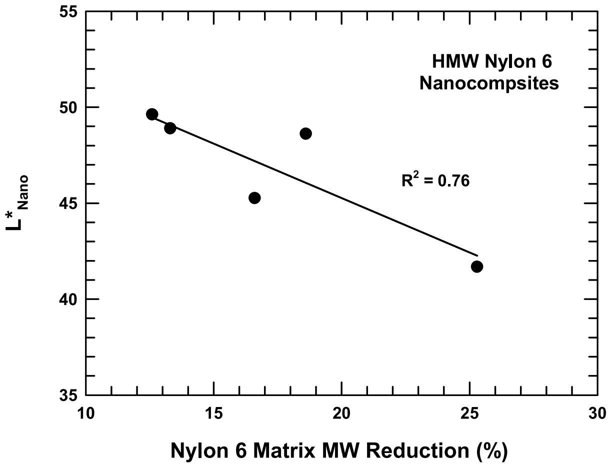

Fig. 13. Relationship between nanocomposite color index and the level of nylon 6 matrix molecular weight experienced during nanocomposite extrusion.

observed with respect to alkyl tail length, since the level of nylon 6 matrix degradation experienced is of the follow order, $(HE)_2M_1R_1 > (HE)_2M_1T_1 > (HE)_2M_1C_1^*$.

Lastly, it should be mentioned that no general correlation exists between the level of platelet exfoliation, as indicated by modulus enhancement, and the extent of color formation. It was shown earlier in the case of one organoclay that the extent of color formation was proportional to the level of platelet exfoliation. In other words, exposing more of the organoclay surface to the polymer leads to deeper color; however, when nanocomposites based on multiple organoclays are compared this relationship does not hold, thus, reiterating that color formation is dependent upon surfactant structure.

Table 5
Molecular weight results for extruded nanocomposites based on $(HE)_2M_1R_1$ organoclay and nylon 6 materials

Material	$\bar{M}_n$[a] (kg/mol)	$\bar{M}_n$ reduction[b] (%)
Virgin HMW	30.1	–
Extruded HMW	28.4	5.6
Extrapolated HMW[c]	26.2	13.0
HMW-$(HE)_2M_1R_1$ nanocomposite	22.5	25.2
Organic chloride of $(HE)_2M_1R_1$ + HMW	20.5	31.9
Model compounds[d]		
trans-7-Tetradecene + HMW	27.3	9.3
cis-9-Heneiocosene + HMW	27.2	9.6
Antioxidants[e]		
$(HE)_2M_1R_1$ + Irganox 1171 + HMW	24.6	18.3
$(HE)_2M_1R_1$ + Irganox 245 + HMW	26.9	10.6
$(HE)_2M_1R_1$ + Wingstay 29 + HMW	26.9	10.6

[a] Molecular weights were determined via intrinsic viscosity measurements.

[b] The percent reduction is relative to the virgin HMW.

[c] Molecular weight corresponding to 0 double bonds in Fig. 6.

[d] Mass of model compound added to HMW nanocomposite was equivalent to the number of double bonds in a $(HE)_2M_1R_1$–nanocomposite containing 3.2 wt% MMT.

[e] The concentration of antioxidant used was 1 wt%.

3.3. Model compound and antioxidant studies

Model compound studies were conducted to further confirm the hypothesis that nylon 6 degradation experienced in nanocomposites is due, as least in part, to the unsaturation in the surfactants in the organoclay. Compounds similar in structure to the unsaturated hydrocarbon substituents of the organoclay modifiers were pre-mixed with HMW nylon 6 and then extruded; Table 5 lists the molecular weight reductions observed. In one case, HMW nylon 6 pellets were coated with the alkyl ammonium chloride of $(HE)_2M_1R_1$ prior to extrusion. The nylon 6 molecular weight loss when this material was extruded is slightly greater than what is experienced in the corresponding HMW-$(HE)_2M_1R_1$ organoclay nanocomposite. The larger decrease may reflect the upper limit of degradation for the HMW-$(HE)_2M_1R_1$ nanocomposite, i.e. the maximum degradation that will occur if all the surfactant in the organoclay is accessible by the nylon 6 i.e. complete organoclay exfoliation. The differences in the counterion a halide vs. a clay platelet, may also affect the extent or pathway of degradation.

A more direct way to verify the role of hydrocarbon tail unsaturation as part of the molecular weight degradation pathway would be to melt mix nylon 6 with long-chain alkenes having double bonds located along the center of the molecule; these molecules should have low volatility to avoid evaporation losses during extrusion. Of the available materials surveyed, *trans*-7-tetradecene (14-carbon) and *cis*-9-henieocene (21 carbon) were the closest matches to these criteria. The reduction of HMW nylon caused by both materials was of the order 9–10% (see Table 5), which is greater than what is experienced by the extrusion of HMW alone, yet less than the degradation seen in the HMW-$(HE)_2M_1R_1$ nanocomposite. The lower level of degradation, however, quite likely reflects the fact that these model compounds have significant volatility at the extrusion temperature; vapors were quite evident during extrusion. With this caveat, these experiments support the proposal of thermo-oxidative degradation stemming from double bonds.

Antioxidants are often added to polymers to minimize degradation during processing. Thus, it was of interest to determine if antioxidants would reduce the nylon 6 molecular weight loss experienced during formation of nanocomposites. Various commercial antioxidants, shown in Fig. 2, were extruded with mixtures of HMW nylon 6 and $(HE)_2M_1R_1$ organoclay. The most effective antioxidants were Irg245 and WS29. Both materials reduced the extent of polyamide MW reduction by more than two-fold. Irg1171, on the other hand, was less effective. Overall, the results are in agreement with the investigations by Lánská [14], who evaluated the influence of various commercial antioxidants on the thermo-oxidative degradation of neat nylon 6.

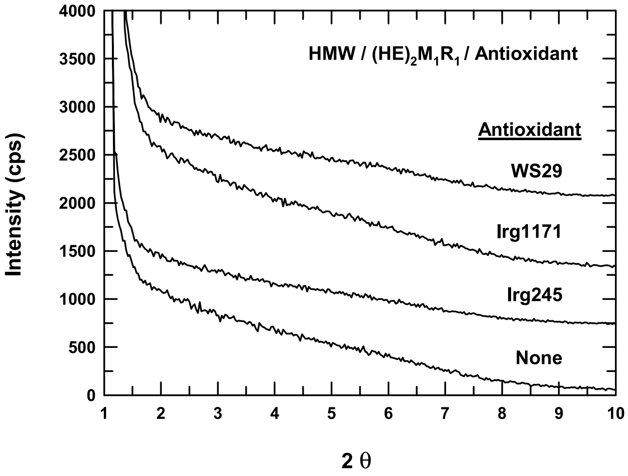

Fig. 14. WAXS curves for HMW nylon 6–$(HE)_2M_1R_1$ nanocomposites with and without antioxidant additives. WAXS scans were conducted in reflection mode on injection molded Izod bars.

Antioxidants based on aromatics diamines, e.g. WS29, were most effective; whereas, phenolic based antioxidants were less effective.

The influence of antioxidants on platelet exfoliation and subsequently, mechanical properties was also evaluated. Fig. 14 shows WAXS results obtained on HMW nylon 6–$(HE)_2M_1R_1$ nanocomposites with and without antioxidant; these are no discernable differences caused by antioxidants. There are no signs of characteristic peaks indicative of intercalated or immiscible clay structures in either case. Furthermore, the antioxidants have no significant effect on mechanical properties, as seen in Table 6; in general, the modulus, yield strength, and elongation at break values fall in line with previously obtained data for HMW nylon 6–$(HE)_2M_1R_1$ nanocomposites. Also, the levels of color formation in the stabilized nanocomposites were approximately the same, or perhaps slightly less, than for the unstablized composites. Thus, reducing the amount degradation via antioxidants does not change the state of exfoliation or any mechanical properties, at a given clay concentration. The changes in molecular weight are not significant enough to affect the matrix properties and degradation does not seem to retard exfoliation of the clay. There is, however, a stronger likehood that mechanical properties will be affected at very high clay concentrations, since more extensive degradation would be expected [5].

4. Conclusions

Polymer matrix degradation and color formation has been documented for nylon 6–organoclay nanocomposites formed by melt processing. The type of nylon 6 material used as well as the chemical structure of the surfactant in the organoclay affects on the extent of polymer degradation and color generation. For a given organoclay, the level of polymer molecular weight reduction and deepness of color was found to be greatest for nanocomposites based on high molecular weight nylon 6 materials; this is attributed to more exposure of the surfactant to the nylon 6, owing to increased levels of organoclay exfoliation.

Changing surfactant structure results in measurable changes in nanocomposite color and polymer matrix molecular weight. Hydroxy–ethyl groups in the surfactant, as opposed to methyl groups, and tallow substituents, as opposed to hydrogenated tallow substituents, produce more nanocomposite color. The latter effect may also be related to the level of polymer degradation experienced during extrusion, i.e. unsaturation in the alkyl ammonium surfactant causes considerable polymer degradation. Although the majority of the degradation is attributed to unsaturation,

Table 6
Effect of antioxidant type on the mechanical properties of HMW nylon 6–$(HE)_2M_1R_1$ organoclay nanocomposites

HMW nylon 6–$(HE)_2M_1R_1$ nanocomposite	Modulus (GPa)	Yield strength (MPa)	Elongation at break (%)	
			Crosshead head speed 0.51 cm/min	Crosshead head speed 5.1 cm/min
No antioxidant				
0.0 wt% MMT	2.75	69.7	304	129
1.6 wt% MMT	3.49	80.4	189	33
3.2 wt% MMT	3.92	84.9	119	27
4.6 wt% MMT	4.59	91.3	39	25
7.2 wt% MMT	5.70	97.6	4.1	6.1
Irg245[a]				
2.6 wt% MMT	3.88	84.5	142	25
Irg1171[a]				
2.7 wt% MMT	3.90	88.1	177	23
WS29[a]				
2.7 wt% MMT	3.96	84.2	152	37
4.2 wt% MMT	4.22	87.6	61	19

[a] The concentration of antioxidant used was 1 wt%.

other causes of degradation may be due to the onium nature of the surfactant and possible hydrolysis. These observations point to the need for more thermally stable surfactants, such as those based on imidazoliums or phosphoniums as suggested by Gilman [33]. Commercial antioxidants, particularly those based on aromatic diamines, are reasonably effective at reducing the amount of degradation of nylon 6 molecular weight experienced during melt extrusion. The extent of exfoliation of the organoclay nor the mechanical properties of the nanocomposite are significantly affected by these chemical processes. Nevertheless, antioxidants may prove beneficial for certain applications particularly where more degradation is expected.

Acknowledgements

This work was supported by the Air Force Office of Scientific Research. The authors would especially like to thank Doug Hunter and Randy Chapman of Southern Clay products for providing organoclay materials, assistance with WAXS measurements, and involvement in numerous insightful discussions. Acknowledgement is also made to Ciba Specialty Chemicals and Goodyear for their donation of antioxidant materials and Honeywell for their generous donation of nylon 6 materials.

References

[1] Xie W, Gao Z, Pan W-P, Hunter D, Singh A, Vaia R. Chem Mater 2001;13(9):2979–90.
[2] Xie W, Gao Z, Liu K, Pan WP, Vaia R, Hunter D, Singh A. Thermochim Acta 2001;367–368:339–50.
[3] VanderHart DL, Asano A, Gilman JW. Macromol 2001;34(12): 3819–22.
[4] VanderHart DL, Asano A, Gilman JW. Chem Mater 2001;13(10): 3796–809.
[5] Matayabas Jr.JC, Turner SR. In: Pinnavaia TJ, Beall GW, editors. Polymer–clay nanocomposites. Chichester, England; New York: Wiley; 2000. p. 207.
[6] Yoon PJ, Hunter DL, Paul DR. Polymer 2003;44(18):5341–54.
[7] Fornes TD, Yoon PJ, Keskkula H, Paul DR. Polymer 2001;42(25): 09929–40.
[8] Fornes TD, Yoon PJ, Keskkula H, Paul DR. Polymer 2002;43(7): 2121–2.
[9] Krishnamoorti R, Vaia RA, Giannelis EP. Chem Mater 1996;8(8): 1728–34.
[10] Cho JW, Paul DR. Polymer 2001;42(3):1083–94.
[11] Krishnamoorti R, Yurekli K. Curr Opin Colloid Interface Sci 2001;6: 464–70.
[12] Fornes TD, Yoon PJ, Hunter DL, Keskkula H, Paul DR. Polymer 2002;43(22):5915–33.
[13] Fornes TD, Paul DR. Polymer 2003;44(14):3945–61.
[14] Lanska B. Polym Degrad Stab 1996;53:89–98.
[15] Tuzar Z, Kratochvil P. J Polym Sci, Lett Ed 1965;3:17.
[16] Oshinski AJ, Keskkula H, Paul DR. Polymer 1996;37(22):4891–907.
[17] Berger-Schunn A. Practical color measurement: a primer for the beginner, a reminder for the expert. New York: Wiley; 1994.
[18] McCreedy K, Keskkula H. Polymer 1975;20:1155–9.
[19] Anderson C, Rodriguez F. Polym Mater Sci Eng 1984;51:608.
[20] Schnabel W. Polymer degradation: principles and practical applications. New York: Hanser Publishers; 1981. p. 186.
[21] Grassie N, Scott G. Polymer degradation and stabilisation. New York: Cambridge University Press; 1985.
[22] Kohen MI, editor. Nylon plastics handbook. New York: Hanser; 1995.
[23] Harding G, MacNulty B. Thermal degradation of polymers. SCI Monograph 13; 1961.
[24] Carey FA. Organic chemistry. New York: McGraw-Hill Inc; 1992.
[25] Davis R, Gilman J, VanderHart D. Polym Degrad Stab 2003;79: 111–21.
[26] Vaia RA, Giannelis EP. Macromolecules 1997;30(25):8000–9.
[27] Vaia RA, Giannelis EP. Macromolecules 1997;30(25):7990–9.
[28] Tanaka G, Goettler LA. Polymer 2002;43(2):541–53.
[29] Fermeglia M, Ferrone M, Pricl S. CASLab online publications, 2002: No. 195 (http://www.caslab.units.it/caslab/).
[30] Fromageot D, Roger A, Lemaire J. Angewandte Makromol Chem 1989;170:71–85.
[31] Karstens T, Rossbach V. Makromol Chem 1990;191(4):757–71.
[32] Li R, Hu X. Polym Degrad Stab 1998;62:523–8.
[33] Gilman JW. Personal communication.